SiNx layers on nanostructured Si solar cells: Effective for optical absorption and carrier collection

Yunae Cho, Eunah Kim, Minji Gwon, Hyeong-Ho Park, Joondong Kim, and Dong-Wook Kim

Citation: Applied Physics Letters **107**, 153101 (2015); doi: 10.1063/1.4933202
View online: http://dx.doi.org/10.1063/1.4933202
View Table of Contents: http://scitation.aip.org/content/aip/journal/apl/107/15?ver=pdfcov
Published by the AIP Publishing

SiN_x layers on nanostructured Si solar cells: Effective for optical absorption and carrier collection

Yunae Cho,[1] Eunah Kim,[1] Minji Gwon,[1] Hyeong-Ho Park,[2] Joondong Kim,[3,a)] and Dong-Wook Kim[1,a)]
[1]*Department of Physics, Ewha Womans University, Seoul 120-750, South Korea*
[2]*Applied Device and Material Lab., Device Technology Division, Korea Advanced Nanofab Center (KANC), Suwon 443270, South Korea*
[3]*Department of Electrical Engineering, Incheon National University, Incheon 406772, South Korea*

(Received 11 July 2015; accepted 2 October 2015; published online 12 October 2015)

We compared nanopatterned Si solar cells with and without SiN_x layers. The SiN_x layer coating significantly improved the internal quantum efficiency of the nanopatterned cells at long wavelengths as well as short wavelengths, whereas the surface passivation helped carrier collection of flat cells mainly at short wavelengths. The surface nanostructured array enhanced the optical absorption and also concentrated incoming light near the surface in broad wavelength range. Resulting high density of the photo-excited carriers near the surface could lead to significant recombination loss and the SiN_x layer played a crucial role in the improved carrier collection of the nanostructured solar cells. © *2015 AIP Publishing LLC*. [http://dx.doi.org/10.1063/1.4933202]

Surface nanostructured arrays can significantly reduce optical reflection of a Si wafer. A graded refractive index, multiple scattering, and the Mie resonance enable remarkable antireflection (AR) effects.[1–8] The optical benefits of such an approach have led to the use of nanopatterned Si wafers for photovoltaic (PV) applications.[1–15] The measured PV performance of nanostructured cells, however, often does not surpass that of conventional cells, despite their substantially improved optical absorption. Electrical losses due to the surface and Auger recombination are considered as the most significant problem to be addressed to increase the power conversion efficiency (PCE) of surface-patterned Si solar cells.[12–15]

In conventional Si solar cells, dielectric coating layers have been used for both AR and passivation purposes.[2,16–20] The PV characteristics of the dielectric-coated Si nanostructured arrays also have been studied.[6,8,12,13] In many of these works, chemical etching techniques were used to prepare random nanostructured arrays. Although such methods are simple and cost-effective in obtaining superior light-trapping at nanostructured Si wafers (so-called 'black Si'), complex processes for doping and dielectric coatings are required to fabricate solar cells due to the extremely small and high-aspect-ratio random features.[12–14] Difficulties in fabrication can lead to deterioration of the performance of nanostructured PV devices, and a clear understanding of the inherent limitations is difficult to obtain. Calculation results of regular nanopatterned arrays can be directly compared with experimental data, which can improve the insight required to inform design strategies to realize high-performance devices.

In this work, we fabricated nanostructured Si solar cells with and without SiN_x dielectric layers, and investigated the PV characteristics of the resulting devices. A quantitative comparison of measured and calculated data allows us to address the following important question: "what considerations are required to optimize the dielectric coating layer on nanostructured Si solar cells, and how does this differ from conventional flat devices?" Our SiN_x-coated nanopatterned cells exhibited a PCE of 15.8%, which is larger than that of the uncoated nanopatterned cells (which exhibited a PCE of 14.0%). The increased quantum efficiency (QE) of the coated cells is attributed primarily to suppression of surface recombination losses, rather than to the AR effects of the SiN_x layer. This suggests that careful surface passivation is more important with nanostructured cells than with planar (i.e., flat, non-patterned) devices.

Si solar cells were fabricated with hexagonal closed-packed arrays of nanoconical frustums patterned using nanoimprint lithography and detailed cell fabrication procedures can be found in our earlier publication.[5] The tapered geometry of the nanocones leads to light trapping at a broader range of wavelengths than when using nanopillars.[7] The geometry of the arrayed frustum nanocones is shown in Fig. 1(a): the top diameter was 120 nm, the bottom diameter was 510 nm, and the height was 320 nm. The center-to-center distance between neighboring features (i.e., pitch) was equal to the bottom diameter (i.e., 510 nm). As shown in Fig. 1(a) and the inset of Fig. 1(b), the periodic nanoconical frustum arrays had a relatively small aspect ratio (i.e., height/diameter), and were regularly spaced with a pitch of ~0.5 μm. Conformal doping and dielectric coating processes are therefore readily available.[5]

Figure 1(b) shows the light current density–voltage (J–V) characteristics and PV parameters of the nanopatterned solar cells with and without an 80-nm-thick SiN_x surface-coating layer. The SiN_x-coated solar cells exhibited a larger short-circuit current density (J_{SC}) and fill factor (FF) than the uncoated devices. The open-circuit voltage (V_{OC}) of the coated nanopatterned cell was slightly smaller than that of the uncoated device. The SiN_x-coated nano-patterned cell exhibited smaller ideality factor than the uncoated cell,[21] indicating suppression of the surface recombination. Thus, cell-to-cell variation in our fabrication processes seems to

a)Electronic addresses: joonkim@incheon.ac.kr and dwkim@ewha.ac.kr

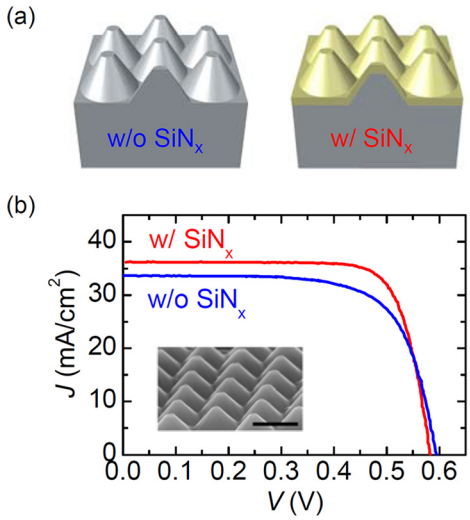

	V_{OC} (V)	J_{SC} (mA/cm2)	FF (%)	PEC (%)
w/o SiN_x	0.595	33.67	70.2	14.0
w/SiN_x	0.583	36.24	74.2	15.8

FIG. 1. (a) A schematic diagram and (b) light current density (J) vs. voltage (V) plot and PV parameters of the Si solar cells with surface-patterned arrays of nanoconical frustums, with and without SiN_x dielectric layers. The inset shows an SEM image of the patterned cell, where the scale bar is 500 nm.

cause the V_{OC} decrease of the coated cell. In spite of the slightly smaller V_{OC}, the PCE of the coated cell is larger than that of the uncoated cell due to improved J_{SC} and FF.

Figure 2 shows the experimental and simulated optical reflectance, R, of several types of cells. Finite-difference time-domain (FDTD) calculations were carried out to obtain the simulation data.[5] The experimental data well agree with the calculation results. Both the nanostructured array and the SiN_x layer led to significant reduction in the optical reflectance of the Si surface. The difference in R due to the nanopatterns and the SiN_x layer coating is denoted ΔR. The gray dashed line in Fig. 2 shows $R[1]-R[2]$, which represents the AR effect of the SiN_x-layer coating. This originates from complete destructive interference. "$R[1]-R[2]$" was maximum at a wavelength of $\lambda \sim 600$ nm, and became negligibly small at $\lambda < 350$ nm. The decrease in the reflectance due to the nanopatterns, "$R[1]-R[3]$," was larger than "$R[1]-R[2]$" over a broad wavelength range. This clearly demonstrates the optical benefits of a nanostructured array.

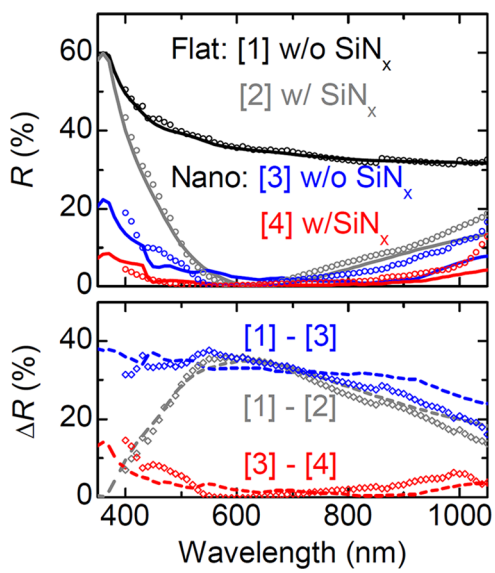

FIG. 2. Experimental (symbols) and calculated (lines) optical reflectance, R, of the flat and nanopatterned cells with and without SiN_x layers, and difference of R (i.e., ΔR) between the cells as a function of wavelength.

The AR effect of the SiN_x layer in the nanopatterned cell exhibited different behaviors compared with that in a flat cell. "$R[1]-R[2]$" was the largest at $\lambda \sim 600$ nm, and became smaller as decreasing or increasing wavelength from 600 nm. "$R[3]-R[4]$" was negligibly small in the wavelength range from 600 nm to 800 nm, and slightly increased as decreasing the wavelength from 600 nm and increasing the wavelength from 800 nm. The presence of a SiN_x layer on the nanopatterned solar cell resulted in a further decrease in R at $\lambda < 600$ nm and $\lambda > 800$ nm. Zhong *et al.* reported that a SiN_x layer increased the scattering cross-section of their Si nanopillars due to modifications to the Mie resonance properties.[8] They also found that the minimum reflectance wavelength of the coated Si nanopillars was determined by not only the destructive interference but also light scattering and interaction with the nanopillars. Similar phenomena may be expected in our nanoconical frustum arrays.[21]

Figure 3 shows the measured external and internal quantum efficiency (EQE and IQE) of the nanopatterned cells with and without the SiN_x layer. Note that the SiN_x layer improved the IQE in very broad wavelength range. In flat cells, the surface recombination loss is supposed to severely deteriorate the carrier collection at short-wavelength region rather than that at long-wavelengths, since the shorter wavelength light has smaller penetration depth than the longer wavelength light. In our flat cells, the IQE gain by the SiN_x layer coating on the flat cells was notable at short wavelengths and became smaller as increasing wavelength.[21] The IQE gain by the SiN_x layer coating on the nanopatterned cells showed distinct wavelength dependence, compared with that on the flat cells. The gain did not show monotonic decrease, while increasing wavelength from 600 nm, and becomes almost zero at $\lambda \sim 1\,\mu$m. The optical penetration depth of the 1-μm-light in Si is as long as hundreds of μm and such long wavelength light can reach the rear side of the flat cell. As a result, the surface passivation by the SiN_x layer

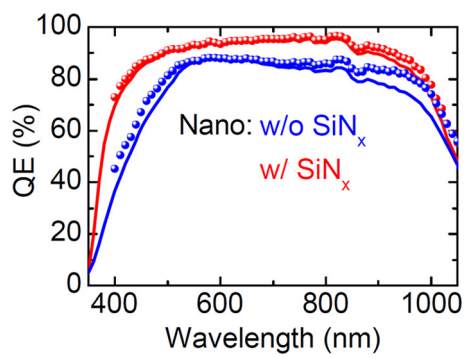

FIG. 3. The EQE (lines) and IQE (symbols) of the nanopatterned cells with (red) and without (blue) SiN_x layers as a function of wavelength.

coating hardly affects the carrier collection probability for such long wavelength light, which should be dominantly determined by the diffusion length of minority carriers.

Figure 4 shows the reverse-biased EQE as a function of voltage for the flat and nanopatterned cells under illumination with short ($\lambda = 450$ nm) and long ($\lambda = 900$ nm) wavelength light. The penetration depths of the 450- and 900-nm-light are 400 nm and 40 μm, respectively. In spite of such a large difference in the penetration depth, IQE gain by the SiN_x layer coating is observed at both wavelengths (Fig. 3). In this regard, 450 nm and 900 nm were chosen as representative wavelengths for short and long wavelength regimes, respectively. The EQE of the uncoated cells (both the flat and nanopatterned cells) increased as the voltage increased, indicating that the recombination losses limited the photocurrent. Furthermore, the EQE exhibited a stronger dependence on voltage in the nanopatterned cell than in the flat cell. The saturation current in the dark depends on the surface recombination velocity;[22,23] this was larger for the uncoated nanopatterned cell than the flat cell by a factor of almost ten.[21] This suggests that the nanostructured cell suffered from serious electrical loss due to the enlarged surface area and surface defect states generated during the patterning process.[23,24] In contrast, the EQE of the SiN_x-coated nanopatterned cell varied little as a function of the applied bias. This shows that the SiN_x layer enabled a sufficiently high charge carrier collection probability and the additional reverse bias hardly affected the EQE.

Figure 5 shows the simulated electric field intensity distributions in the cells under illumination with 450-nm and 900-nm light. The intensity in the flat cells exhibited an exponential decrease with increasing depth into the cells. This decrease was more gradual at longer wavelengths, due to the larger penetration depth of Si. The surface nanostructures act as nanocavities for Mie resonance, resulting in strong field confinement near the surface, as shown in Figs. 5(c) and 5(d).[6–8] As a result, the light intensity at the surface of the nanopatterned cells was much larger than that of the flat cell even at $\lambda = 900$ nm. It follows that a lager fraction of the photogenerated carriers will be present near to the surface of the nanopatterned cells. At the uncoated Si surface, such a high concentration of charge carriers will

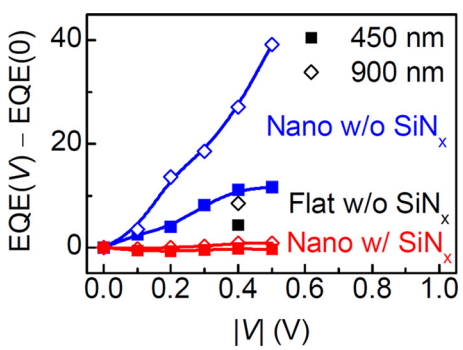

FIG. 4. Reverse-bias voltage dependence of the EQE for the flat and nanopatterned cells with and without SiN_x layers. The filled squares indicate the data at a wavelength $\lambda = 450$ nm and the open diamonds at $\lambda = 900$ nm. The blue symbols correspond to the uncoated nanopatterned cell, the black symbols to the uncoated flat cell, and the red symbols to the SiN_x-coated nanopatterned cell.

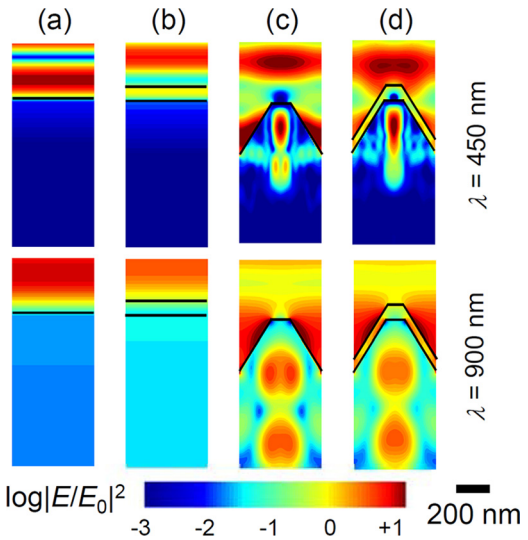

FIG. 5. Simulated electric field distributions in (a) the uncoated flat cell, (b) the SiN_x-coated flat cell, (c) the uncoated nanopatterned cell, and (d) the SiN_x-coated nanopatterned cell. The top four figures correspond to illumination with 450-nm light, and the bottom four figures to illumination with 900-nm light. The black lines show the surface and the SiN_x/Si interface of the cells.

result in serious recombination loss, due to the defect states and upward band bending.[12–22] Thus, the SiN_x passivation in the nanopatterned cell significantly improved the carrier collection efficiency at both short and long wavelengths, as shown in Fig. 4.

Assuming a carrier collection probability of 100%, we may calculate the maximum achievable short-circuit current density using the following equation:

$$J_{SC,\text{calculated}} = \int_{300nm}^{\lambda_g} I(\lambda)\frac{e\lambda}{hc}d\lambda,$$

where λ is the wavelength, $A(\lambda)$ is the optical absorption, $I(\lambda)$ is the AM 1.5 solar spectral irradiance, e is the electron charge, h is Planck's constant, c is the speed of light, and λ_g is the wavelength corresponding to the optical band gap of Si.[5,25] Figure 6 shows the calculated and measured J_{SC} values of the flat and nanopatterned cells with and without SiN_x dielectric layers. The red and blue areas in Fig. 6 represent J_{SC} gain due to the AR effects of the SiN_x coating and the nanopatterns, respectively. For all the cells, the measured J_{SC} was less than $J_{SC,\text{calculated}}$, and the difference between the two is attributed to carrier collection losses. For the flat cells, the interference AR effects of the SiN_x coating significantly increased $J_{SC,\text{calculated}}$ from 27.77 to 39.09 mA/cm^2 (with a difference of $\Delta J_{SC,\text{calculated}} = 11.32$ mA/cm^2). The measured J_{SC} of the SiN_x-coated and uncoated flat cells were 34.02 mA/cm^2 and 25.42 mA/cm^2, respectively, giving $\Delta J_{SC} = 8.60$ mA/cm^2. For the nanopatterned cells, the SiN_x coating only slightly increased $J_{SC,\text{calculated}}$ from 41.33 mA/cm^2 to 42.37 mA/cm^2, ($\Delta J_{SC,\text{calculated}} = 1.04$ mA/cm^2), as the SiN_x-mediated increase in the optical absorption was small (see "[3]–[4]" in Fig. 2). The measured value of J_{SC} for the SiN_x-coated nanopatterned cells was 36.24 mA/cm^2, and that for the uncoated nanopatterned cell was 33.67 mA/cm^2. The difference of 2.57 mA/cm^2 exceeds $\Delta J_{SC,\text{calculated}}$ by a factor of more than 2. This suggests that the increase in the photocurrent due to the SiN_x layer on

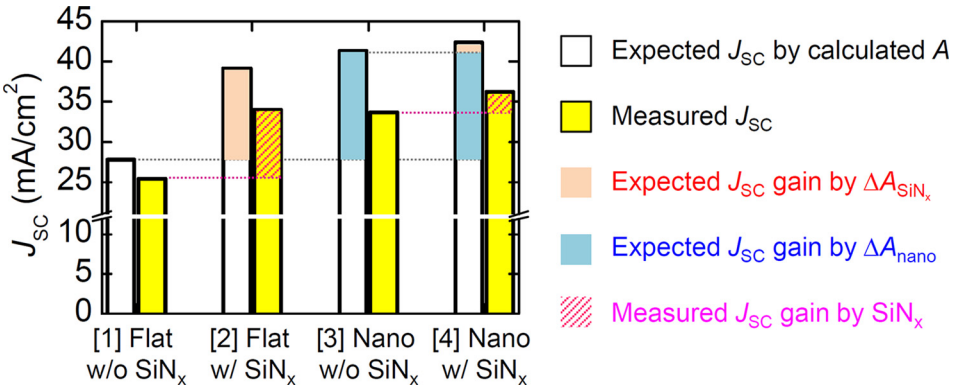

FIG. 6. Calculated and measured J_{SC} of the flat and nanopatterned solar cells with and without SiN_x layers.

the nanopatterned cell resulted mainly from the improved collection efficiency of the photogenerated carriers, rather than increased optical absorption.

We investigated the PV characteristics of the solar cells with hexagonal arrays of nanofrustums, with and without SiN_x dielectric layers. The PCE of the coated nanopatterned cell was 15.8%, which was higher than that of the uncoated nanopatterned cell (i.e., 14.0%). The SiN_x layer coating improved the carrier collection efficiency of the nanopatterned cells at both short and long wavelengths, whereas such coating usually helped carrier collection of the flat cells only at short wavelengths. The Mie resonance in the nanostructures significantly increased the density of the photogenerated carriers near the surface even at long wavelengths. Such high density of charge carriers near the Si surface may lead to large recombination losses. Therefore, proper surface passivation via the deposition of a dielectric layer is crucial to exploit the enhanced optical absorption of the nanostructured solar cells.

This work was supported by Korea Institute of Energy Technology Evaluation and Planning Grant (KETEP-20133030011000). Y.C., E.K., M.G., and D.K. were also supported by the National Research Foundation of Korea Grant (No. 2015001948).

[1]M. Algasinger, J. Paye, F. Werner, J. Schmidt, M. S. Brandt, M. Stutzmann, and S. Koynov, Adv. Energy Mater. **3**, 1068 (2013).
[2]H. K. Raut, V. A. Ganesh, A. S. Nair, and S. Ramakrishna, Energy Environ. Sci. **4**, 3779 (2011).
[3]J. Zhu, Z. Yu, G. F. Burkhard, C.-M. Hsu, S. T. Connor, Y. Xu, Q. Wang, M. McGehee, S. Fan, and Y. Cui, Nano Lett. **9**, 279 (2009).
[4]A. Mavrokefalos, S. E. Han, S. Yerci, M. S. Branham, and G. Chen, Nano Lett. **12**, 2792 (2012).
[5]Y. Cho, M. Gwon, H.-H. Park, J. Kim, and D.-W. Kim, Nanoscale **6**, 9568 (2014).
[6]P. Spinelli, M. A. Verschuuren, and A. Polman, Nat. Commun. **3**, 692 (2012).
[7]Z. Y. Wang, R. J. Zhang, S. Y. Wang, M. Lu, X. Chen, Y. X. Zheng, L. Y. Chen, Z. Ye, C. Z. Wang, and K. M. Ho, Sci. Rep. **5**, 7810 (2015).
[8]S. Zhong, Y. Zeng, Z. Huang, and W. Shen, Sci. Rep. **5**, 8915 (2015).
[9]S. Jeong, M. D. McGehee, and Y. Cui, Nat. Commun. **4**, 2950 (2013).
[10]J.-H. Yun, E. Lee, H.-H. Park, D.-W. Kim, W. A. Anderson, J. Kim, N. M. Litchinitser, J. Zeng, J. Yi, M. M. D. Kumar, and J. Sun, Sci. Rep. **4**, 6879 (2014).
[11]J. Kim, J.-H. Yun, H. Kim, Y. Cho, H.-H. Park, M. M. D. Kumar, J. Yi, W. A. Anderson, and D.-W. Kim, Sci. Rep. **5**, 9256 (2015).
[12]Y. Liu, T. Lai, H. Li, Y. Wang, Z. Mei, H. Liang, Z. Li, F. Zhang, W. Wang, A. Y. Kuznetsov, and X. Du, Small **8**, 1392 (2012).
[13]J.-W. Song, J.-Y. Jung, H.-D. Um, X. Li, M.-J. Park, Y.-H. Nam, S.-M. Shin, T. J. Park, R. B. Wehrspohn, and J.-H. Lee, Adv. Mater. Interfaces **1**, 1400010 (2014).
[14]J. Oh, H.-C. Yuan, and H. M. Branz, Nat. Nanotechnol. **7**, 743 (2012).
[15]F. Toor, H. M. Branz, M. R. Page, K. M. Jones, and H.-C. Yuan, Appl. Phys. Lett. **99**, 103501 (2011).
[16]R. Hezel and K. Jaeger, J. Electrochem. Soc. **136**, 518–523 (1989).
[17]T. Lauinger, J. Schmidt, A. G. Aberle, and R. Hezel, Appl. Phys. Lett. **68**, 1232 (1996).
[18]M. Vetter, Thin Solid Films **337**, 118 (1999).
[19]J. Sritharathikhun, C. Banerjee, M. Otsubo, T. Sugiura, H. Yamamoto, T. Sato, A. Limmanee, A. Yamada, and M. Konagai, Jpn. J. Appl. Phys. **46**, 3296 (2007).
[20]V. V. Iyengar, B. K. Nayak, and M. C. Gupta, Sol. Energy Mater. Sol. Cells **94**, 2251 (2010).
[21]See supplementary material at http://dx.doi.org/10.1063/1.4933202 for dark current-voltage characteristics of the nanopatterned cells, calculated optical reflectance spectra of the nanopatterned cells, quantum efficiency data of the flat cells, and schematic band diagrams of uncoated and coated cells.
[22]M. A. Green, *Solar cells: Operating Principles Technology and System Applications* (Prentice-Hall, New Jersey, 1982).
[23]E. Lee, Y. Kim, M. Gwon, D.-W. Kim, S.-H. Baek, and J. H. Kim, Sol. Energy Mater. Sol. Cells **103**, 93 (2012).
[24]F. F. Corpuz, Jr., T. Matsumoto, W.-B. Kim, and H. Kobayashi, ECS Solid State Lett. **1**, P89 (2012).
[25]J. Kim, E. Lee, M. Ju, H. Kim, J. Yi, S.-J. Moon, M. S. Hyun, and D.-W. Kim, Opt. Express **21**, A607 (2013).